Available online at www.sciencedirect.com

SCIENCE DIRECT

Tectonophysics 394 (2004) 221–232

TECTONOPHYSICS

www.elsevier.com/locate/tecto

Crustal and mantle strengths in continental lithosphere: is the jelly sandwich model obsolete?

Juan Carlos Afonso*, Giorgio Ranalli

Department of Earth Sciences and Ottawa-Carleton Geoscience Centre, Carleton University, 1125 Colonel By Drive, Ottawa, Canada K1S 5B6

Received 15 August 2003; accepted 20 August 2004
Available online 27 October 2004

Abstract

The relative importance of the contribution of the lower crust and of the lithospheric mantle to the total strength of the continental lithosphere is assessed systematically for realistic ranges of layer thickness, composition, and temperature. Results are presented as *relative strength maps*, giving the ratio of the lower crust to upper mantle contribution in terms of crustal thickness and surface heat flow. The lithosphere shows a "jelly sandwich" rheological layering for low surface heat flow, thin to average crustal thickness, and felsic or wet mafic lower crustal compositions. On the other hand, most of the total strength resides in the seismogenic crust in regions of high surface heat flow, crust of any thickness, and dry mafic lower crustal composition.

Keywords: Continental lithosphere; Strength; Composition; Rheology; Relative strength maps

1. Introduction

The strength of the lithosphere (i.e. the total force per unit width necessary to deform a lithospheric section at a given strain rate) is a function of composition, crustal thickness, and geotherm. Rheological layering is a consequence of compositional layering (Ranalli and Murphy, 1987). The prevailing model (commonly referred to as the "jelly sandwich model") to explain lithospheric features has been for several years that of a strong upper crust overlying a soft lower crust and a strong uppermost mantle (cf., among others, Ranalli and Murphy, 1987; Ranalli, 1995; Cloetingh and Burov, 1996; Watts and Burov, 2003). In this model, a significant part of the total strength resides in the lithospheric mantle, except when the geothermal gradient is very high, which causes both lower crust and mantle to be soft. Recently, however, Maggi et al. (2000a,b) and Jackson (2002) have suggested that most of the strength in many continental areas resides in the upper seismogenic crust, and that in some places the lower crust may be stronger than the upper mantle

* Corresponding author. Tel.: +1 613 5202600x4392; fax:+1 613 5202569.
E-mail addresses: jcarlos@ccs.carleton.ca (J.C. Afonso), granalli@ccs.carleton.ca (G. Ranalli).

0040-1951/$ - see front matter © 2004 Elsevier B.V. All rights reserved.
doi:10.1016/j.tecto.2004.08.006

(see also discussion in De Meer et al., 2002). These conclusions are based on the scarcity of earthquakes in the continental mantle, and on the correlation between effective elastic thickness and seismogenic thickness in several continental areas. This model relies on water as a weakening agent in the upper mantle, while the lower crust is simply assumed to be hydrous or dry, depending on the lack or presence of seismicity.

In this paper, we systematically explore the relative total (integrated) strength of lower crust and upper mantle as a function of composition, geotherm, and thickness. We use a three-layer compositional lithospheric model (upper crust, lower crust, and lithospheric mantle), and type geotherms (parameterised in terms of surface heat flow) obtained from an analytical solution to the heat conduction equation. The new concept of *relative strength map* is introduced to represent the relative contribution of lower crust and lithospheric mantle to total lithospheric strength in terms of crustal thickness and surface heat flow.

2. Mechanical behaviour of the lithosphere

It is commonly accepted that, to the first order, the mechanical behaviour of the lithosphere can be modelled using experimental constraints on rock rheology (cf., e.g. Ranalli and Murphy, 1987; Kohlstedt et al., 1995; Ranalli, 2003), although there are some dissenting voices (Burov, 2003).

The brittle regime for most rocks can be adequately described by the Coulomb frictional law, which in the case of pre-existing faults of favourable orientation and negligible cohesion can be written as (Sibson, 1974)

$$\sigma_1 - \sigma_3 = \alpha\rho g z(1-\lambda) \quad (1)$$

where $\sigma_1-\sigma_3$ is the maximum stress difference; α is a numerical factor depending on friction coefficient and fault type; ρ is the average density of rocks above the depth z, and λ is the pore fluid factor (ratio of pore fluid pressure to lithostatic pressure). The most uncertain parameter is the pore fluid pressure, although it has been shown that it is often near-hydrostatic down to depths of ~12 km (Zoback and Townend, 2001). In the absence of information regarding specific regions, we take α=3.0 (thrust faulting) and a typical ("hydrostatic") value λ=0.4.

Table 1
Creep parameters for lithospheric rocks

Lithology	A [MPa^{-n} s^{-1}]	n	E [kJ mol^{-1}]	References
Quartzite (wet)	3.2×10^{-4}	2.3	154	1
Felsic granulite	8.0×10^{-3}	3.1	243	2
Mafic granulite	1.4×10^{4}	4.2	445	2
Maryland diabase (dry)	8.0	4.7	485	3
"Undried" diabase (wet)	2.0×10^{-4}	3.4	260	4
Peridotite (dry)	2.5×10^{4}	3.5	532	5
Peridotite (wet)	2.0×10^{3}	4.0	471	5, 6

(1) Kirby and Kronenbrg (1987); (2) Wilks and Carter (1990); (3) Mackwell et al. (1998); (4) Shelton and Tullis (1981); (5) Chopra and Paterson (1984); (6) Chopra and Paterson (1981).

In the ductile regime, we assume power-law dislocation creep, which results in a creep strength given by (cf., e.g. Ranalli, 1995)

$$\sigma_1 - \sigma_3 = \left(\frac{\dot{\varepsilon}}{A}\right)^{\frac{1}{n}} \exp\left(\frac{H}{nRT}\right), \quad H = E + PV \quad (2)$$

where $\dot{\varepsilon}$ is the steady-state strain rate, T temperature in degrees Kelvin, P pressure, R the universal gas constant, H the creep activation enthalpy, E the activation energy, V the activation volume, and n and A material creep parameters. When modelling lithospheric behaviour, the pressure dependence of creep can be neglected, as it is small at pressures pertaining to the lithosphere ($V\sim 10^{-6}$ m^3 mol^{-1}). The creep parameters for the various materials used to derive relative strength maps are listed in Table 1.

3. Calculation of geotherms

The rheological behaviour and the total strength of the lithosphere in a particular area are strongly dependent on the assumed geotherm. Since we are interested in exploring variations of rheology for a range of general conditions, we assume here that heat transfer by advection is negligible and that steady-state conditions apply, which is reasonable for areas where the latest tectonothermal episode occurred at times $\gtrsim$100 Ma. Hence, we estimate type geotherms by solving the steady-state, 1-D heat conduction equation with radiogenic heat production for three-layer lithospheric models of different thickness and composition, with surface boundary condition $T_o = 15$ °C, and continuity of both temperature and gradient at internal interfaces. The solution is

$$T(z) = -\frac{A_1 z^2}{2K_1} + [Q_m + (z_2 - z_1)A_2 + A_1 z_1]\frac{z}{K_1} + T_o\,, \qquad z_o < z < z_1 \tag{3a}$$

$$T(z) = -\frac{A_2 z^2}{2K_2} + \left[\frac{z_1 A_2}{K_2} + \frac{Q_m}{K_1} + \frac{A_2(z_2 - z_1)}{K_1}\right]z + \frac{z_1^2}{2}\left(\frac{A_1}{K_1} - \frac{A_2}{K_2}\right) + T_o\,, \qquad z_1 < z < z_2 \tag{3b}$$

$$T(z) = -\frac{A_3 z^2}{2K_3} + \left[z_2\left(\frac{A_3}{K_3} - \frac{A_2}{K_2}\right) + \frac{z_1 A_2}{K_2} + \frac{Q_m}{K_1} + \frac{A_2(z_2 - z_1)}{K_1}\right]z + T(z_2) + z_2^2\left(\frac{A_2}{K_2} - \frac{A_3}{2K_3}\right) - z_2\left[\frac{z_1 A_2}{K_2} + \frac{Q_m}{K_1} + \frac{A_2(z_2 - z_1)}{K_1}\right], \quad z > z_2 \tag{3c}$$

where A_1, A_2, A_3 and K_1, K_2, K_3 are volumetric heat production rates (HPR) and thermal conductivities in the upper crust, lower crust, and lithospheric mantle, respectively; Q_m is the heat flowing across the Moho (mantle heat flow), z_1 and z_2 are the depths to the bottom of the upper crust and Moho, respectively; and $T(z_2)$ is the temperature at the Moho given by Eq. (3b). As expected, Eq. (3c) differs only slightly from a straight line, due to the low radiogenic heat production in the mantle.

In contrast to oceanic crust, where HPR and compositional variations are negligible, continental crust usually shows a considerable variation in composition and enrichment in radiogenic elements. The most important factors controlling the shape of the geotherm in the continental crust are (i) tectono-thermal age, (ii) HPR distribution at different levels, (iii) thermal conductivity, and (iv) mantle heat flow (i.e. heat flow across the Moho). However, (ii) and (iii) are intimately related to rock composition and they can be modelled as a function of the lithologies assumed in the crustal section (Clauser and Huenges, 1995; Kukkonen and Lahtinen, 2001).

Values of heat production, thermal conductivity, and density used in the calculations are given in Table 2. Volumetric heat production rates, compatible with the chosen lithology are estimated from the empirical relation (Rybach, 1988)

$$A = 10^{-5}\rho(3.48C_K + 2.56C_{Th} + 9.52C_U) \tag{4}$$

where C_K is the potassium concentration in weight percent, C_{Th} and C_U are the thorium and uranium concentrations in ppm, respectively, and ρ is the density in kg m^{-3}. Concentrations of radio-elements are obtained from several references included in Table 2.

The relative effects of temperature and pressure on the value of K depend on the particular geotherm and depth; but usually the pressure effect can be ignored within the lithosphere without introducing significant errors (Chapman and Furlong, 1992). The temperature dependence of thermal conductivity in the upper crust is estimated from the relation (Zoth and Haenel, 1988)

$$K(T) = 0.7 + 770/(350 + T(z)) \tag{5}$$

where T is in °C. In the lower layers, constant values of thermal conductivity are chosen, as

Table 2
Thermophysical parameters for different lithologies used in this work

Layer	A [μW m^{-3}]	K [W m^{-1} K^{-1}]	Density [kg m^{-3}]	References
Upper crust (wet quartzite)	1.4	2.5 at surface[a]	2640	1, 2, 3, 4
Lower crust (felsic granulite)	0.4–0.5	2.1	2750	1, 2, 3,4, 5, 6, 10
Lower crust (mafic granulite)	0.25–0.4	2.1	2880	1, 2, 3,4, 5, 8, 10
Lower crust (dry diabase)	0.4	2.1	2850	2, 3, 4, 7, 10
Lower crust (wet diabase)	0.4	2.1	2850	2, 3, 4, 7, 10
Lithospheric mantle (peridotite)	0.006	3.0	3320	1, 2, 4, 9

(1) Kukkonen and Lahtinen (2001); (2) Zoth and Haenel (1988); (3) Clauser and Huenges (1995); (4) Olhoeft and Johnson (1989); (5) Ray et al. (2003); (6) Louden et al. (2000); (7) Van Schmus (1989); (8) Höltä et al. (2000); (9) Ranalli (1995); (10) Christensen and Mooney (1995).

[a] K decreases in the upper crust following Eq. (5).

conductivities of different rocks tend to converge at $T > 400$ °C (e.g. Zoth and Haenel, 1988; Clauser and Huenges, 1995).

The mantle heat flow Q_m appearing in Eqs. (3a,b,c) can be estimated from the relation

$$Q_o = Q_m + Q_R\,, \quad Q_R = \sum_{i=1}^{i=n} A_i \Delta z_i \qquad (6)$$

where Q_o is the surface heat flow (SHF), Q_m is the mantle heat flow across the Moho, Q_R is the radiogenic heat production in the crust, and A_i and Δz_i are HPR and thickness of the nth layer, respectively. To avoid unrealistically high or low mantle heat flow values, we have constrained Q_m to the range of values inferred in areas of similar thickness and HPR. Generally, typical values of Q_m vary from ~20% to ~80% of surface heat flow (e.g. Nyblade and Pollack, 1993; Jaupart and Mareschal, 1999; Artemieva and Mooney, 2001; Ray et al., 2003). The mantle heat flow (Q_m) is here restricted to maximum values of ~35 mW m^{-2}. Although the latter is higher than most estimates for stable regions (between ~11 and 18 mW m^{-2}, e.g. Jaupart and Mareschal, 1999; Kukkonen and Lahtinen, 2001), it is in agreement with some estimates in Paleozoic orogens and Precambrian provinces (Artemieva and Mooney, 2001; Ray et al., 2003). For the range of thicknesses, SHF, and HPR considered in this work, Eq. (6) can be used to parameterise Eq. (3a,b,c) as a function of Q_o and Q_R without assuming unrealistic values for Q_m.

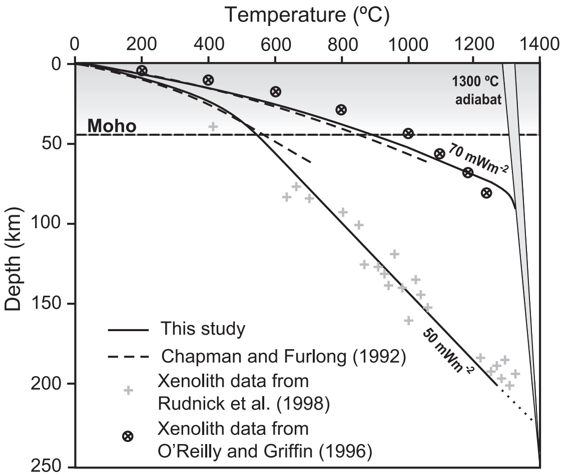

Fig. 1. Geotherms for two different SHF and given lithology (see text), compared with xenolith data. Thermophysical parameters are listed in Table 2.

As an example, two lithospheric geotherms, calculated from Eq. (3a,b,c) for SHF of 50 and 70 mW m^{-2}, are shown in Fig. 1. In both cases, a 20-km-thick upper crust (wet quartzite) overlies a 25-km-thick lower crust (felsic granulite) and a peridotitic mantle (thermophysical parameters are listed in Table 2). For comparison, geotherms obtained by Chapman and Furlong (1992) for the same SHF are also shown, together with xenolith data from the Siberian, South African, and Tanzanian cratons (SHF ~50 mW m^{-2}; Rudnick et al., 1998), and from a hotter palaeogeotherm (perhaps with an advective component) from Southeastern Australia (O'Reilly and Griffin, 1996).

4. Effects of composition

Rheological models of the continental lithosphere are strongly dependent on the assumed composition. Information about the composition of continental lithosphere comes essentially from three different sources: (a) seismic data (e.g. Christensen and Mooney, 1995; Kennett and van der Hilst, 1998; Brown et al., 2003), (b) petrology of surface exposures (e.g. Vissers et al., 1997; Kern et al., 1999; Trommsdorff et al., 2000; Zhai et al., 2001), and (c) xenolith data (e.g. Rudnick, 1992; O'Reilly and Griffin, 1996; Zhang et al., 1998; Condie, 1999; Schmitz and Bowring, 2003; Yu et al., 2003). Any rheological model of the lithosphere must be consistent with these fundamental observations. The upper continental crust composition is usually dominated by granitoids, quartz-rich sediments, and quartz-bearing schists. Alkali feldspars can be major constituents in granitic rocks as well as in some gneisses. However, although dislocation creep is effective in feldspars at temperatures ≥500 °C, these minerals rarely form a stress-supporting framework (Stöckhert and Renner, 1998), and quartz is generally the phase controlling the bulk rheology of the upper continental crust. Since in most tectonic environments the upper crust is hydrated, the creep parameters of wet quartzite are probably the best approximation (rheological and thermophysical parameters are listed in Tables 1 and 2). However, the rheological properties of the upper crust do not affect the arguments presented here.

The composition of the lower crust is less constrained, being mainly controlled by observation of seismic velocities and comparison with experimental data. The expected dominant lithology depends on several variables such as geothermal gradient, thickness of the total crust, tectonic history, and composition of the parental material. The bulk of the continental lower crust generally has seismic velocities compatible with mafic composition (mafic granulite; Christensen and Mooney, 1995). However, it has been shown that more felsic compositions (commonly felsic granulites) may predominate in particular regions (e.g. Christensen and Mooney, 1995; Gao et al., 1998; Stöckhert and Renner, 1998; Brown et al., 2003). In order to cover a range of possibilities, we model its rheological behaviour using the creep parameters of both mafic and felsic granulites, and also of wet and dry diabase. We do not include the often assumed plagioclase rheology (cf., e.g. Ranalli, 2000), since it is practically undistinguishable from the wet diabase rheology used here.

There is an extensive bibliography dealing with the composition and rheology of the mantle (cf., e.g. Karato and Wu, 1993; Jackson, 1998; Ranalli, 1998, 2001, and references therein). Geophysical, petrological, and theoretical evidence support an ultramafic upper mantle composed mainly of olivine, pyroxenes, and garnet. Since olivine is by far the volumetrically dominant phase (>50%), many experimental studies have been performed on plasticity of natural and synthetic olivine aggregates (see Ranalli, 2001 for references).

Two unresolved questions concern the predominant creep mechanism and the hydration state. The creep mechanism has been discussed, among others, by Karato and Wu (1993), Wu (1999), and Ranalli (1998, 2001). In the stress range associated with plate movements (1–100 MPa), power-law creep is likely to be predominant. This conclusion is supported by the occurrence of seismic anisotropy (Karato and Wu, 1993).

The problem regarding the fluid content in the upper mantle is even more poorly understood. The mantle composition includes fluids such as water and carbon dioxide (cf., e.g. Yamamoto et al., 2002; Xu et al., 2003). Various estimates for the average water content of the mantle yield values ranging from 40 to 1000 ppm (e.g. Bell and Rossman, 1992; Thompson, 1992; Hegner and Vennemann, 1997), while amounts of only about ~200 ppm are needed to produce a significant reduction in the strength of olivine aggregates (Chopra and Paterson, 1984). However, the mechanisms of weakening (intra- or intergranular) and the manner in which water resides in mantle rocks are still unclear (cf., e.g. Mackwell et al., 1985; Drury and Fitzgerald, 1998). The occurrence of water expands the stress-grain size field in which power-law creep predominates (Karato et al., 1986). There are indications that a wet rheology may be appropriate for continental lithospheric mantle in zones recently affected by subduction of oceanic lithosphere and post-Paleozoic tectonothermal events, while a dry rheology may be more relevant for older regions. For these reasons, we use power-law creep parameters for both dry and wet peridotite to model mantle strength.

5. Relative strength maps

For the rheological modelling, we assume an upper crust of constant thickness (20 km) overlying a lower crust of variable thickness (from 10 to 40 km). The total lithospheric thickness is not predetermined, but given by the depth at which the creep strength of the upper mantle falls below 5 MPa. SHF values in continents typically vary between 40 and $\gtrsim$80 mW m^{-2}, although lower and higher values have been measured in some Precambrian shields and active regions, respectively (e.g Jaupart and Mareschal, 1999; Artemieva and Mooney, 2001). Since we are particularly interested in the transition where the lower crust becomes “stronger” than the upper mantle, we allow SHF to vary between 50 and 75 mW m^{-2}. Values <50 mW m^{-2} always give lower crusts “weaker” than upper mantle, except in the extreme case of dry diabase-wet peridotite combination (see below), whereas values $\gtrsim$70 mW m^{-2} are associated with active regions where steady-state conditions do not apply.

The total strengths of lower crust (SLC) and of lithospheric mantle (SLM) are obtained by integration of Eqs. (1) and (2)

$$SLC = \frac{\alpha\rho_{\mathrm{lc}}g(1-\lambda)}{2}({z_1'}^2 - {z_1}^2) + \left(\frac{\dot{\varepsilon}}{A}\right)^{\frac{1}{n}} \int_{z_1'}^{z_2} \exp\left(\frac{E}{nRT(z)}\right) \mathrm{d}z \tag{7a}$$

$$SLM = \frac{\alpha\rho_{\mathrm{um}}g(1-\lambda)}{2}({z_2'}^2 - {z_2}^2) + \left(\frac{\dot{\varepsilon}}{A}\right)^{\frac{1}{n}} \int_{z_2'}^{z_3} \exp\left(\frac{E}{nRT(z)}\right) \mathrm{d}z \tag{7b}$$

where z_1 is the depth to the top of the lower crust, z_1' is the depth to the brittle–ductile transition in the lower crust (if present), z_2 is the depth of the Moho, z_2' is the depth to the brittle–ductile transition in the upper mantle (if present), z_3 is the depth to the bottom of the mechanical lithosphere, ρ_{lc} and ρ_{um} are the densities of lower crustal and upper mantle rocks, and $T(z)$ is the temperature distribution (given by Eqs. (3b) and (3c)).

The ratio SLC/SLM is plotted in Fig. 2 on *relative strength maps* giving contour lines of the ratio as a function of crustal thickness and SHF for various crustal and mantle rheologies. For common ranges of temperature and strain rate, the dependence of SLC/SLM on the latter can be neglected (provided strain rates are equal in lower crust and upper mantle), since the decrease/increase in the creep strength due to a decrease/increase in the strain rate is proportional in both layers. For example, for mafic granulite, felsic granulite, and wet diabase, a change in strain rate from 10^{-15} to 10^{-13} s^{-1} only gives variations of ~0.07, 0.004, and 0.003, respectively, in the SLC/SLM ratio. This allows strength-ratio maps to be used, to the first order, for different strain rates. Only in the case of an extremely strong lower crust (dry diabase), the dependence on strain rate becomes more important, especially at very low SHF and low crustal thicknesses.

It should be noted that the SLC/SLM ratio represents the relative importance of the lower crustal and upper mantle contributions to total lithospheric strength, which may not be directly related to the strength ratio of lower crustal and upper mantle rocks at the Moho. In other words, it is possible that the local creep strength of crustal material is less than that of mantle material at the Moho (for instance, for quartz- or plagioclase-controlled rheologies; Ranalli, 2000), while the relative strength ratio defined in this paper is >1. Also, a constant crustal composition within a given map does not imply that an increase in the SHF is due only to an increase in the mantle heat flow, except for a constant crustal thickness, since the radiogenic heat production in the crust also varies with the thickness of the crust as indicated in Eq. (6).

If an upper crust with a constant thickness of 30 km is used instead of 20 km, the magnitude of the contour lines decreases by about one order of magnitude, but the general pattern remains. This is an obvious consequence of reducing the thickness of the lower crust in the model. A quartz-dominated upper crust thicker than 30 km is unrealistic and therefore not considered here.

A few general conclusions can be drawn from the maps. Low SHF and low values of crustal thickness increase the relative importance of the mantle contribution to total lithospheric strength. This is partly a consequence of the fact that under these conditions the uppermost mantle may be brittle (although there are high uncertainties related to the extrapolation of the frictional criterion to upper mantle pressures; cf. Ranalli, 1995). The effects of composition are equally important. The combination of a hard lower crust (mafic granulite or dry diabase) and a soft mantle (wet peridotite) results in SLC/SLM>1 for practically all conditions. However, if the mantle is dry, this result is valid only for a limited range of crustal thickness and SHF (≥35–40 km and 55–65 mW m^{-2}, respectively). On the other hand, a felsic or

Fig. 2. Relative strength maps for various lower crust and upper mantle compositions. Curves of constant SLC/SLM values are plotted as continuous lines. Rheology: (A) felsic granulite/dry peridotite; (B) felsic granulite/wet peridotite; (C) mafic granulite/dry peridotite; (D) mafic granulite/wet peridotite; (E) wet diabase/dry peridotite; (F) wet diabase/wet peridotite; (G) dry diabase/dry peridotite; (H) dry diabase/wet peridotite. Rheological and thermophysical parameters are listed in Tables 1 and 2.

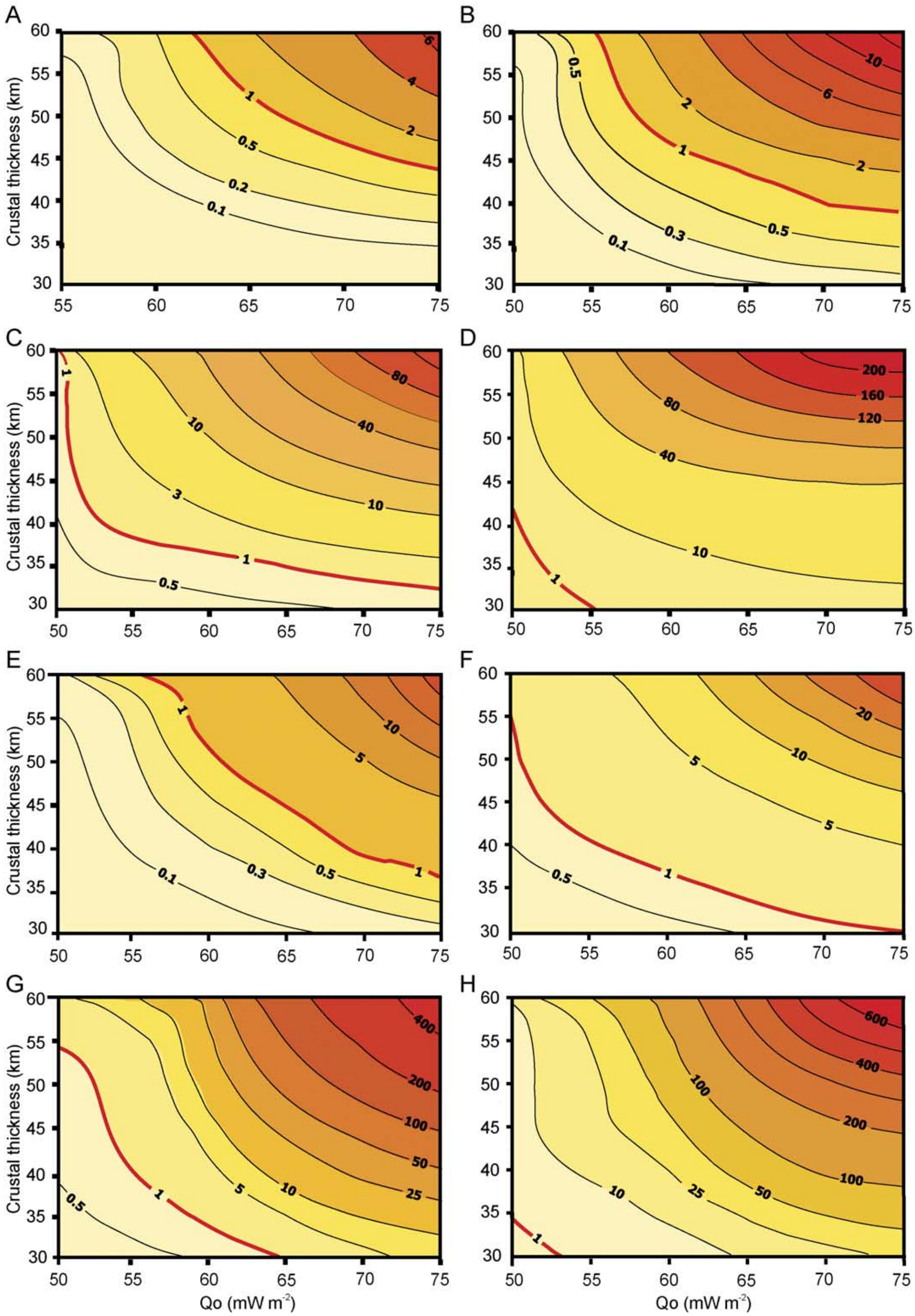
A
B
C
D
E
F
G
H
Crustal thickness (km)
Qo (mW m^{-2})
6
4
2
1
0.5
0.2
0.1
10
0.3
80
40
3
200
160
120
20
5
400
100
50
25
600

wet mafic lower crust results in SLC/SLM<1 for most realistic values of SHF and crustal thickness, with only small differences introduced by the state of the mantle.

Composition, thickness, and temperature combine in a complex way. The general "topography" of relative strength maps is also affected by the relative importance of frictional and power-law terms in Eq. (7a). With increasing SHF, the brittle–ductile transition migrates to shallower depths, and the frictional term may vanish. Moreover, as a consequence of varying creep parameters for each particular lithology, the exponential terms in Eq. (7a) and (7b) result in a complex non-linear behaviour of the SLC/SLM ratio.

The lower crustal thickness plays an important role in the relative strength in two different ways. The first and most obvious one is that thicker layers have more material with similar rheological properties to resist stresses. The second effect is related to the displacement of the Moho to deeper levels, and consequently to higher temperatures. Lithospheric mantle becomes relatively soft (e.g. strengths on the order of ~10^{10}–10^{9} N m^{-1} for dry and wet peridotite, respectively) for Moho depths of ~55 km and SHF of ~65–70 mW m^{-2}. Both of the above effects tend to increase the SLC/SLM ratio by increasing and decreasing the lower crust and upper mantle strengths, respectively. Areas of thickened crust, such as continental collisional zones, usually have relatively high SHF (e.g. Himalayas; Zagros). Hence, it is expected that in these zones, the lithospheric mantle does not contribute significantly to the total strength of the lithosphere, even if a "dry" peridotite rheology is assumed. Fig. 3 illustrates some of these complications. It shows "sections" across relative strength maps, giving the strength ratio as a function of SHF for selected crustal thicknesses and two rheological end-member cases. It can be seen that the dependence of the ratio on SHF is non-linear and different in the two cases. Fig. 3A shows a typical concave-upward "section" across relative strength-maps representative of the "jelly sandwich model", where exponential terms in Eq. (7a) and (7b) control the value of the SLC/SLM ratio. In contrast, for a strong lower crust/soft upper mantle combination (Fig. 3B), the profile is commonly

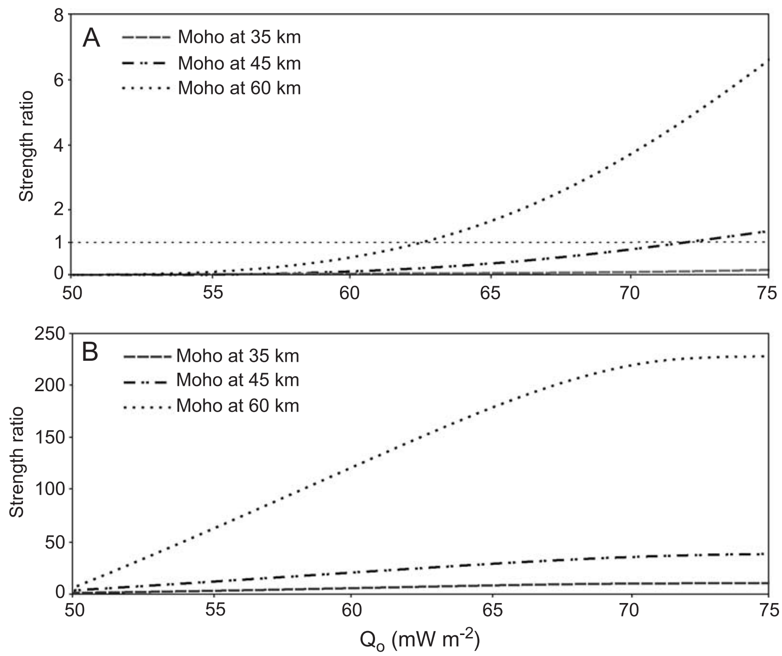

Fig. 3. Sections across relative strength maps for different crustal thicknesses. Rheology: (A) felsic granulite/dry peridotite; the dashed horizontal line marks the value SLC/SLM=1; (B) mafic granulite/wet peridotite; SLC/SLM>1 practically everywhere.

slightly convex-upward, reflecting the relative importance of the linear term in Eq. (7a) and (7b) for low to moderate SHF.

The ratio SLC/SLM is an indication of the relative contributions of lower crust and upper mantle to total lithospheric strength, but an assessment of the resistance to deformation of the lithosphere requires knowledge of the latter as well. Table 3 lists values of total strengths for lower crust and lithospheric mantle for the different lithologies utilized in this work. Individual values are listed for several combinations of SHF and crustal thickness to serve as a general guide in reading strength-ratio maps. For completeness, the total strength of the upper crust is also shown.

6. Conclusions

For many years, the accepted model to explain the rheological behaviour of the continental lithosphere has been that of a strong upper crust overlying a soft lower crust and a stronger (under most conditions) upper mantle. This model, based on experimental

Table 3
Total strength values [N m^{-1}] for lower crust and lithospheric mantle as a function of SHF and crustal thickness. The integrated strength of the upper crust is included in the first row for comparison

Crustal thickness (km)	Surface heat flow (mW m^{-2})			
	50	60	70	
Upper crust (wet quartzite)				
20[a]	2.6×10^{12}	1.7×10^{12}	1.3×10^{12}	
Mafic granulite				
35	1.3×10^{13}	6.77×10^{12}	1.0×10^{12}	Lower crust
45	1.44×10^{13}	5.0×10^{12}	7.0×10^{11}	
60	1.5×10^{13}	5.17×10^{12}	5.6×10^{11}	
35	3.6×10^{13} (1.6×10^{13})	1.7×10^{13} (9.9×10^{11})	6.6×10^{11} (9.7×10^{10})	Mantle ( ) wet
45	1.7×10^{13} (4.2×10^{12})	9.9×10^{11} (2.0×10^{11})	4.5×10^{10} (1.8×10^{10})	
60	3.1×10^{13} (4.2×10^{12})	2.3×10^{11} (4.3×10^{10})	8.4×10^{9} (3.2×10^{9})	
Felsic granulite				
35	6.0×10^{11}	2.4×10^{11}	3.6×10^{10}	Lower crust
45	6.8×10^{11}	1.8×10^{11}	3.8×10^{10}	
60	7.3×10^{11}	1.9×10^{11}	4.1×10^{10}	
35	3.6×10^{13} (2.0×10^{13})	1.4×10^{13} (1.2×10^{12})	7.4×10^{11} (9.9×10^{10})	Mantle ( ) wet
45	4.8×10^{13} (5.7×10^{12})	1.2×10^{12} (2.4×10^{11})	5.3×10^{10} (2.1×10^{10})	
60	8.7×10^{13} (1.2×10^{13})	3.8×10^{11} (6.6×10^{10})	1.1×10^{10} (4.1×10^{9})	
Dry diabase				
35	2.0×10^{13}	1.6×10^{13}	7.17×10^{12}	Lower crust
45	4.7×10^{13}	2.0×10^{13}	7.5×10^{12}	
60	4.68×10^{13}	2.0×10^{13}	7.6×10^{12}	
35	5.3×10^{13} (1.6×10^{13})	1.3×10^{13} (1.7×10^{12})	6.5×10^{11} (1.4×10^{11})	Mantle ( ) wet
45	5.1×10^{13} (6.7×10^{12})	2.8×10^{12} (5.0×10^{11})	1.2×10^{11} (4.3×10^{10})	
60	3.5×10^{13} (4.4×10^{12})	6.7×10^{11} (1.7×10^{11})	2.4×10^{10} (1.3×10^{10})	
Wet diabase				
35	4.3×10^{12}	1.2×10^{12}	2.6×10^{11}	Lower crust
45	4.8×10^{12}	1.3×10^{12}	2.8×10^{11}	
60	5.1×10^{12}	1.3×10^{12}	2.9×10^{11}	
35	5.3×10^{13} (1.6×10^{13})	1.3×10^{13} (1.7×10^{12})	6.5×10^{11} (1.4×10^{11})	Mantle ( ) wet
45	5.1×10^{13} (6.7×10^{12})	2.8×10^{12} (5.0×10^{11})	1.2×10^{11} (4.3×10^{10})	
60	3.5×10^{13} (4.4×10^{12})	6.7×10^{11} (1.7×10^{11})	2.4×10^{10} (1.3×10^{10})	

[a] Thickness of upper crust for estimation of upper crustal rheology (first row); total thickness of crust for all other cases.

rheology, has proven to be quite useful in accounting for various lithospheric processes (e.g. flexure; cf. Burov and Diament, 1992; Ranalli, 1995; Watts, 2001). However, this "jelly sandwich" picture has been challenged, mainly on the basis of the depth distribution of continental earthquakes, and it has been proposed that most of the lithospheric strength resides in the upper (seismogenic) crust, and that the upper mantle may be softer than the lower crust (Maggi et al., 2000a,b; Jackson, 2002, see also discussion in De Meer et al., 2002).

In this paper, we have attempted to elucidate the range of applicability of these two different models by examining various theoretical scenarios in terms of lithospheric structure, composition, and temperature conditions. The results, presented in Fig. 2 as relative strength maps, can be summarized as follows:

– A metasomatized, water-rich upper mantle underlying a mafic lower crust (especially if dry) results in SLC/SLM>1; this outcome is emphasized by large crustal thicknesses and high SHF.
– A volatile-depleted upper mantle underlying a felsic lower crust results in SLC/SLM<1, especially for low-to-moderate crustal thicknesses and SHF.

The first set of conditions may apply to some Phanerozoic lithospheres recently affected by subduction, mantle metasomatism, and/or collisional events (e.g. Himalayas, Zagros). In these areas, the upper mantle contribution to total lithospheric strength should be low or negligible. The second set of conditions may be more appropriate for older orogens (Lower Paleozoic–Proterozoic) and Precambrian Shields.

Although the problem of a "jelly sandwich" model vs. a "seismogenic crust only" model for the continental lithosphere is far from being completely solved, our main conclusion is that neither has general applicability. Lithospheres with different compositions and tectonothermal histories have different rheological properties, and should be modelled accordingly. Future studies taking into account the tectonothermal evolution, local conditions, and actual tectonic setting in diverse regions are needed to obtain information about the spatial and temporal variability of mechanical properties in continental lithosphere. Perhaps we should begin thinking in terms of a *world map of lithopheric strength.*

Acknowledgements

We thank J. Blenkinsop and F. Devine who provided helpful reviews of a preliminary version of this paper. We also thank R. Albert and J.C. Mareschal for valuable comments and suggestions. This work has been supported by Carleton University and OGS (Ontario Graduate Scholarship) PhD scholarships to JCA and an NSERC (Natural Sciences and Engineering Research Council of Canada) discovery grant to GR.

References

Artemieva, I.M., Mooney, W.D., 2001. Thermal thickness and evolution of Precambrian lithosphere: a global study. J. Geophys. Res. 106, 16387–16414.

Bell, D.R., Rossman, G.R., 1992. Water in Earth's mantle: the role of nominally anhydrous minerals. Science 255, 1391–1397.

Brown, D., Carbonell, R., Kukkonen, I., Ayala, C., Golovanova, I., 2003. Composition of the Uralide crust from seismic velocity (V_p, V_s), heat flow, gravity, and magnetic data. Earth Planet. Sci. Lett. 6621, 1–17.

Burov, E.B., 2003. The upper crust is softer than dry quartzite. Tectonophysics 361, 321–326.

Burov, E.B., Diament, M., 1992. Flexure of the continental lithosphere with multilayer rheology. Geophys. J. Int. 109, 449–468.

Chapman, D.S., Furlong, K.P., 1992. Thermal state of the continental lower crust. In: Fountain, D.M., Arculus, R., Kay, R.W. (Eds.), Continental Lower Crust. Elsevier, Amsterdam, pp. 179–199.

Chopra, P.N., Paterson, M.S., 1981. The experimental deformation of dunite. Tectonophysics 78, 453–473.

Chopra, P.N., Paterson, M.S., 1984. The role of water in the deformation of dunite. J. Geophys. Res. 89, 7861–7876.

Christensen, N.I., Mooney, W.D., 1995. Seismic velocity structure and composition of the continental crust: a global view. J. Geophys. Res. 100, 9761–9788.

Clauser, C., Huenges, E., 1995. Thermal conductivity of rocks and minerals. In: Ahrens, T.J. (Ed.), Rock Physics and Phase Relations: A Handbook of Physical Constants, AGU Reference Shelf, vol. 3, pp. 105–126.

Cloetingh, S., Burov, E.B., 1996. Thermomechanical structure of European continental lithosphere: constraints from rheological profiles and EET estimates. Geophys. J. Int. 124, 695–723.

Condie, K.C., 1999. Mafic crustal xenoliths and the origin of the lower continental crust. Lithos 46, 95–101.

De Meer, S., Drury, M.R., De Bresser, J.H.P., Pennock, G.M., 2002. Current issues and new developments in deformation mechanisms, rheology and tectonics. In: De Meer, S., et al. (Eds.), Deformation Mechanisms, Rheology and Tectonics: Current Status and Future Perspectives, Special Publication - Geological Society of London vol. 200, pp. 1–27.

Drury, M.R., Fitzgerald, J.D., 1998. Mantle rheology: insights from laboratory studies of deformation and phase transition. In: Jackson, I. (Ed.), The Earth's Mantle—Composition, Structure, and Evolution. Cambridge Univ. Press.

Gao, S., Zhang, B.R., Jin, Z.M., Kern, H., Luo, T.C., Zhao, Z.D., 1998. How mafic is the lower crust? Earth Planet. Sci. Lett. 161, 101–117.

Hegner, E., Vennemann, T.W., 1997. Role of fluids in the origin of Tertiary European intraplate volcanisms: evidence from O, H, and Sr isotopes in melilites. Geology 25, 1035–1038.

Hölttä, P., Huhma, H., Mänttäri, I., Peltonen, P., Juhanoja, J., 2000. Petrology and geochemistry of mafic granulite xenoliths from the Lahtojoki kimberlite pipe, eastern Finland. Lithos 51, 109–133.

Jackson, I. (Ed.), 1998. The Earth's Mantle-Composition, Structure, and Evolution. Cambridge Univ. Press.

Jackson, J.A., 2002. Strength of the continental lithosphere: time to abandon the jelly sandwich? GSA Today 12, 4–10.

Jaupart, C., Mareschal, J.C., 1999. The thermal structure and thickness of continental roots. Lithos 48, 93–114.

Karato, S.I., Wu, P., 1993. Rheology of the upper mantle: a synthesis. Science 260, 771–778.

Karato, S.I., Paterson, M.S., FitzGerald, J.D., 1986. Rheology of synthetic olivine aggregates: influence of grain size and water. J. Geophys. Res. 91, 8176–9151.

Kennett, B.L.N., van der Hilst, R.D., 1998. Seismic structure of the mantle: from subduction zone to craton. In: Jackson, I. (Ed.), The Earth's Mantle-Composition, Structure, and evolution. Cambridge Univ. Press, pp. 381–404.

Kern, H., Gaob, S., Jin, Z., Popp, T., Jin, S., 1999. Petrophysical studies on rocks from the Dabie ultrahigh-pressure (UHP) metamorphic belt, Central China: implications for the composition and delamination of the lower crust. Tectonophysics 301, 191–215.

Kirby, S.H., Kronenbrg, A.K., 1987. Rheology of the lithosphere: selected topics. Rev. Geophys. 25, 1219–1244.

Kohlstedt, D.L., Evans, B., Mackwell, S.J., 1995. Strength of the lithosphere: Constraints imposed by laboratory experiments. J. Geophys. Res. 100, 17587–17602.

Kukkonen, I.T., Lahtinen, R., 2001. Variation of radiogenic heat production rate in 2.8–1.8 Ga old rocks in the central Fennoscandian shield. Phys. Earth Planet. Inter. 126, 279–294.

Louden, K.E., Withmarsh, R.B., Mareschal, J.-C., 2000. Data report: measurements of radiogenic heat production on basement samples from Sites 1067 and 1068. In: Beslier, M.-O., Withmarsch, R.B., Wallace, P.J., Girardeau, J. (Eds.), Proc. ODP, Sci. Results, vol. 173, pp. 1–4. Online.

Mackwell, S.J., Kohlstedt, D.L., Paterson, M.S., 1985. The role of water in the deformation of olivine single crystals. J. Geophys. Res. 90, 11319–11333.

Mackwell, S.J., Zimmerman, M.E., Kohlstedt, D.L., 1998. High-temperature deformation of dry diabase with application to tectonics on Venus. J. Geophys. Res. 103, 975–984.

Maggi, A., Jackson, J.A., Priestley, K., Baker, C., 2000a. A re-assessment of focal depth distributions in southern Iran, the Tien Shan and northern India: do earthquakes really occur in the continental mantle? Geophys. J. Int. 143, 629–661.

Maggi, A., Jackson, J.A., McKenzie, D., Priestley, K., 2000b. Earthquake focal depths, effective elastic thickness, and the strength of the continental lithosphere. Geology 28, 495–498.

Nyblade, A.A., Pollack, H.N., 1993. A global analysis of heat flow form Precambrian terrains: implications for the thermal structure of the Archean and Proterozoic lithosphere. J. Geophys. Res. 98, 12207–12218.

O'Reilly, S.Y., Griffin, W.L., 1996. 4-D lithosphere mapping: methodology and examples. Tectonophysics 262, 3–18.

Olhoeft, G.R., Johnson, G.R., 1989. Densities of rocks and minerals. In: Carmichael, R.S. (Ed.), Practical Handbook of Physical Properties of Rocks and Minerals. CRC Press, pp. 141–176.

Ranalli, G., 1995. Rheology of the Earth (2nd ed.). Chapman & Hall.

Ranalli, G., 1998. Inferences on mantle rheology from creep laws. In: Wu, P. (Ed.), Dynamics of the Ice Age Earth—A Modern Perspective. TransTech Publications, Zurich, pp. 323–340.

Ranalli, G., 2000. Rheology of the crust and its role in tectonic reactivation. J. Geodyn. 30, 3–15.

Ranalli, G., 2001. Mantle rheology: radial and lateral viscosity variation inferred from microphysical creep laws. J. Geodyn. 32, 425–444.

Ranalli, G., 2003. How soft is the crust? Tectonophysics 361, 319–320.

Ranalli, G., Murphy, D.C., 1987. Rheological stratification of the lithosphere. Tectonophysics 132, 281–295.

Ray, L., Kumar, P.S., Reddy, G.K., Roy, S., Rao, G.V., Srinivasan, R., Rao, U.M., 2003. High mantle heat flow in a Precambrian granulite province: evidence from southern India. J. Geophys. Res. 108 (B2), 2084.

Rudnick, R.L., 1992. Xenoliths—Samples of the lower continental crust. In: Fountain, D.M., Arculus, R., Kay, R.W. (Eds.), Continental Lower Crust. Elsevier, Amsterdam, pp. 269–316.

Rudnick, R.L., McDonough, W.F., O'Connell, R.J., 1998. Thermal structure, thickness and composition of continental lithosphere. Chem. Geol. 145, 395–411.

Rybach, L., 1988. Determination of heat production rate. In: Haenel, R., Rybach, L., Stegena, L. (Eds.), Handbook of Terrestrial Heat-Flow Density Determination. Kluwer Academic Publishers, Dordrecht, pp. 125–142.

Schmitz, M.D., Bowring, S.A., 2003. Constraints on the thermal evolution of continental lithosphere from U–Pb accessory mineral thermochronometry of lower crustal xenoliths, Southern Africa. Contrib. Mineral Petrol. 144, 592–618.

Shelton, G., Tullis, J., 1981. Experimental flow laws for crustal rocks (abstract). EOS Trans. AGU 62, 396.

Sibson, R.H., 1974. Frictional constraints on thrust, wrench and normal faults. Nature 249, 542–544.

Stöckhert, B., Renner, J., 1998. Rheology of crustal rocks at ultrahigh pressure. In: Hacker, B.R., Liou, J.G. (Eds.), When Continents Collide: Geodynamics and Geochemistry of Ultrahigh-Pressure Rocks. Kluwer Academic Publishers, pp. 57–95.

Thompson, A.B., 1992. Water in the Earth's upper mantle. Nature 358, 295–302.

Trommsdorff, V., Hermann, J., Müntener, O., Pfiffner, M., Risold, A.C., 2000. Geodynamic cycles of subcontinental lithosphere in the Central Alps and the Arami enigma. J. Geodyn. 30, 77–92.

Van Schmus, W.R., 1989. Radioactivity properties of minerals and rocks. In: Carmichael, R.S. (Ed.), Practical Handbook of Physical Properties of Rocks and Minerals. CRC Press, pp. 585–596.

Vissers, R.L.M., Drury, M.R., Newman, J., Fliervoet, T.F., 1997. Mylonitic deformation in upper mantle peridotites of the North Pyrenean Zone (France): implications for strength and strain localization in the lithosphere. Tectonophysics 279, 303–325.

Watts, A.B., 2001. Isostasy and the flexure of the lithosphere. Cambridge Univ. Press.

Watts, A.B., Burov, E.B., 2003. Lithospheric strength and its relationship to the elastic and seismogenic layer thickness. Earth Planet. Sci. Lett. 213, 113–131.

Wilks, K.R., Carter, N.L., 1990. Rheology of some continental lower crustal rocks. Tectonophysics, 57–77.

Wu, P., 1999. Modelling postglacial sea level with power law rheology and a realistic ice model in the absence of ambient tectonic stress. Geophys. J. Int. 139, 691–702.

Xu, X., O'Reilly, S.H., Griffin, W.L., Zhou, X., 2003. Enrichment of upper mantle peridotite: petrological, trace element and isotopic evidence in xenoliths from SE China. Chem. Geol. 174, 1–26.

Yamamoto, J., Kagi, H., Kaneoka, I., Lai, Y., Prikhod'ko d, V.S., Arai, S., 2002. Fossil pressures of fluid inclusions in mantle xenoliths exhibiting rheology of mantle minerals: implications for the geobarometry of mantle minerals using micro-Raman spectroscopy. Earth Planet. Sci. Lett. 198, 511–519.

Yu, J.H., Xu, X., O'Reilly, S.Y., Griffin, W.L., Zhang, M., 2003. Granulite xenoliths from Cenozoic Basalts in SE China provide geochemical fingerprints to distinguish lower crust terranes from the North and South China tectonic blocks. Lithos 67, 77–102.

Zhai, M.G., Guo, J.H., Liu, W.J., 2001. An exposed cross-section of early Precambrian continental lower crust in North China Craton. Phys. Chem. Earth 26, 781–792.

Zhang, M., Zhou, X.H., Zhang, J.B., 1998. Nature of the lithospheric mantle beneath NE China: evidence from potassic volcanic rocks and mantle xenoliths. In: Flower, M.F.J., et al. (Eds.), Mantle Dynamics and Plate Interactions in East Asia, AGU, Geodynamics Series, vol. 27, pp. 197–219.

Zoback, M.D., Townend, J., 2001. Implications of hydrostatic pore pressures and high crustal strength for the deformation of intraplate lithosphere. Tectonophysics 336, 19–30.

Zoth, G., Haenel, R., 1988. Thermal conductivity. In: Haenel, R., Rybach, L., Stegena, L. (Eds.), Handbook of Terrestrial Heat Flow Density Determination. Kluwer Academic Publishers, pp. 449–453.